CHAPTER

The power of ultra-high field for cognitive neuroscience: Gray-matter optimized fMRI

25

Serge O. Dumoulin[a,b,c,d] **and Tomas Knapen**[a,b,c]

[a]*Spinoza Centre for Neuroimaging, Amsterdam, The Netherlands* [b]*Computational Cognitive Neuroscience and Neuroimaging, Netherlands Institute for Neuroscience, Amsterdam, The Netherlands* [c]*Experimental and Applied Psychology, Vrije Universiteit Amsterdam, Amsterdam, The Netherlands* [d]*Experimental Psychology, Utrecht University, Utrecht, The Netherlands*

Highlights

- 7T MRI has greatly improved sensitivity and specificity.
- Gray-matter optimized (GMO) fMRI balances sensitivity and specificity at UHF.
- GMO fMRI confronts traditional data-analysis assumptions.
- GMO fMRI reorients experiments toward individuals and local neural computations.
- UHF forces a paradigm shift toward high-SNR measurements in single individuals.

25.1 Introduction

The human brain holds the key to who we are, our memories, thoughts, and perception of the world around us. The goal of cognitive neuroscience is to explain how these mental processes arise from neural computations. Since the discovery of functional MRI more than 30 years ago, the promise has been its ability to measure the response properties of populations of neurons inside the living human brain. As such, it has powered a revolution in cognitive neuroscience. Even in popular culture, the concept of localized brain function has placed our minds firmly inside our heads. Ultra-high field (UHF) MRI imaging at magnetic field strengths of 7 Tesla or more stands to push the envelope in terms of our measurement capabilities. But these more powerful measurements at UHF also reveal limitations of engrained paradigms of experimentation and analyses. So, how should we as cognitive neuroscientists wield this new, powerful tool? In this chapter, we outline how ongoing developments in the field of UHF imaging may prompt a paradigm change in cognitive neuroscience.

The most basic advantage of increased field strengths is increased signal-to-noise ratios (SNRs). The MRI signal and fMRI response scale superlinearly with field strength (Yacoub et al., 2001; Uludağ et al., 2009). This means that when cognitive neuroscientists move to UHF from standard field strengths such as 3 Tesla, they can expect a rough fourfold improvement in the efficacy of their measurements (Cai et al., 2021). Moreover, the spatial point-spread function is more narrow at UHF, meaning that our measurements are not only more sensitive, but also inherently more spatially specific than at lower field strengths. One popular avenue of research is to let the improvements in

Advances in Magnetic Resonance Technology and Applications. Volume 10. ISSN 2666-9099. https://doi.org/10.1016/B978-0-323-99898-7.00012-2

sensitivity go toward higher spatial resolutions and to bring the mesoscopic scale of cortical columns and layers into view (as discussed in Chapter 24). Here in this chapter, however, we assert a much more readily available and more powerful gain for cognitive neuroscience: whole-brain fMRI experiments of the type that are now customarily conducted at a field strength of 3 Tesla. This assertion is supported by the fact that an impressive wave of impactful recent findings has resulted from this specific use of UHF fMRI, an observation we draw from in this chapter.

We focus on whole-brain functional MRI in this chapter because (1) it is the most readily available tool for cognitive neuroscientists and (2) it has proven to be the most productive tool in the last few years. In separate boxes, we highlight the unique potential of UHF for in-vivo histology (Box 25.1), laminar and columnar fMRI (Box 25.2), and functional spectroscopy (Box 25.3). However, all of these applications have several significant still-unresolved challenges that limit, for now, their usefulness for the cognitive neuroscience community at large.

25.2 What is the optimal spatial resolution from a cognitive neuroscience perspective?

If the goal of the fMRI experiment is not to image cortical columns or layers, but to examine whole-brain responses to certain stimuli and tasks, what is the optimal resolution? From an MR physics perspective, it is common to describe signal quality in terms of a trade-off between thermal noise and physiological noise. The chosen resolution determines which of the two noise sources is dominant, with smaller voxels being dominated by thermal noise whereas larger voxels are physiological-noise-dominated. The optimal resolution is then where the two are balanced. However, when reasoning about the optimal fMRI resolution from a cognitive neuroscientist's perspective, a similar trade-off along the dimension of voxel size exists—but it is defined by different factors. As shown in Fig. 25.1, these factors are *spatial specificity* and *effective SNR*. By sampling smaller tissue volumes, higher resolutions

BOX 25.1 PUSHING ANATOMICAL MRI TOWARD INDIVIDUAL-LEVEL IN-VIVO HISTOLOGY

The cortex consists of different layers or laminae that differ in cyto- and myeloarchitecture. These laminar differences were the basis of the well-known cortical area parcellations of Brodmann based on post-mortem histology (Brodmann, 1909). Whereas the Brodmann areas were based on differences in cytoarchitecture, contemporaries Vogt and Vogt based their area definitions on histological differences in myeloarchitecture (Vogt and Vogt, 1919). Beyond the cortex, also subcortical nuclei and cerebellum contain subdivisions differencing in cyto- and myeloarchitecture. These structural differences support different functions of the brain. The Brodmann areas are still used today, though the laminar organizations that define the Brodmann areas are not visible on conventional MRI.

The resolution of anatomical images at UHF is high enough to start resolving these laminar differences. Furthermore, together with recent developments toward the efficient and often simultaneous collection of multiple MRI contrasts (see also Chapter 14) provides different clues about the underlying laminar architecture (Caan et al., 2018; Fracasso et al., 2016; Weiskopf et al., 2013). The higher resolution thus affords researchers the possibility to sample tissue properties at different cortical depths, providing diverse clues regarding local histological organization, i.e., in-vivo histology.

In-vivo histology has the potential to define cortical areas in individuals providing a new anatomical reference frame for function, inter-participant alignment, or disease biomarkers. For instance, localization of the stria of Gennari allows the anatomical delineation of the primary visual cortex even in the blind (Trampel et al., 2011). Though there is a lot of potential in in-vivo histology, there are several strides to be made in data-acquisition and data-analysis strategies. This makes in-vivo histology not an off-the-shelf technique for cognitive neuroscientists, but certainly a promising avenue.

BOX 25.2 IMAGING A NEW ORGANIZATION SCALE: LAMINAR AND COLUMNAR FMRI

***Laminae*:** The laminae of the cortex differ in their connectivity and function. For example, thalamocortical connections arrive primarily in central (granular) layers (Felleman and Essen, 1991). Hence, the granular layers are most prominent in primary sensory cortices and nearly absent in motor cortices. Likewise, supra- and infragranular layers are thought to contain predominantly corticocortical and subcortical/corticospinal connections, respectively. Cortical laminae therefore contain unique information on the information flow in the brain.

***Columns*:** In a cortical column, neurons with similar functions are grouped together across cortical depth. Columns are well established in early visual cortex and somatosensory cortices. In the primary visual cortex, different columnar structures (such as ocular dominance and orientation) are organized in such a way that all combinations repeat themselves. This has led to the notion of a hypercolumn or cortical processing unit (Hubel and Wiesel, 1977; Mountcastle et al., 1957). Moreover, between-area connections are often columnar (Jones et al., 1975). Columns are often hypothesized to exist across the brain, although the generality of this principle is uncertain (Horton and Adams, 2005). For example, the columnar structure of the primary visual cortex is not always present across species.

The resolution of functional images at UHF is high enough to start to resolve these laminar columnar functional structures (see also Chapter 24). Ultimately, this could provide a window into the information flow within the cortex and the hypothesized cortical processing unit. Although there is a lot of effort and interest in laminar and columnar imaging, there are passionate debates in the field on the different data-acquisition techniques (see Chapter 23), different data-analysis strategies, fine-scale link of the fMRI signal to the underlying physiology, and the correct interpretation of the results. This makes laminar and columnar fMRI not an off-the-shelf technique for cognitive neuroscientists, but certainly a promising avenue.

BOX 25.3 TOWARD DIRECT MEASURES OF BRAIN ACTIVITY: FUNCTIONAL MR SPECTROSCOPY

Magnetic resonance spectroscopy (MRS) quantifies the regional biochemistry composition in the living human brain (see also Chapter 26). In most studies, MRS is a steady-state measurement that reflects the concentrations of various compounds, for example, the neurotransmitter glutamate or GABA. The increased SNR of UHF enables not only steady-state measures, but also tracking, for example, glutamate modulations over time as a function of cognitive tasks, i.e., functional MRS (Stanley and Raz, 2018). Unlike functional MRI, functional spectroscopy may yield a more direct measure of neural activity and likely less sensitivity to vascular changes. Although there is a lot of potential in functional MRS, there are still several strides to be made in the development of robust data acquisition techniques and data-quantification methods. Furthermore, a lot is currently unknown about the nature of the glutamate changes over time and how these changes should be interpreted, necessitating work into the exact underlying mechanisms that are verified by direct neurophysiological measurements in animal models.

increase the specificity of the neural populations sampled by our voxels, i.e., sampling only gray matter as opposed to a mix of gray matter, white matter, and CSF. The latter of these two factors, effective SNR, more akin to contrast-to-noise than signal-to-noise in classical MR terms, can be seen as related to the amount of explainable variance in the fMRI signal time course, or its *noise ceiling*. These two factors compete, since any increase in spatial resolution increases spatial specificity but decreases effective SNR roughly as a function of voxel volume. We argue that for cognitive neuroscience experiments, the goal is to balance these two countervailing factors to optimize the detection of localized responses of neuronal populations in gray matter.

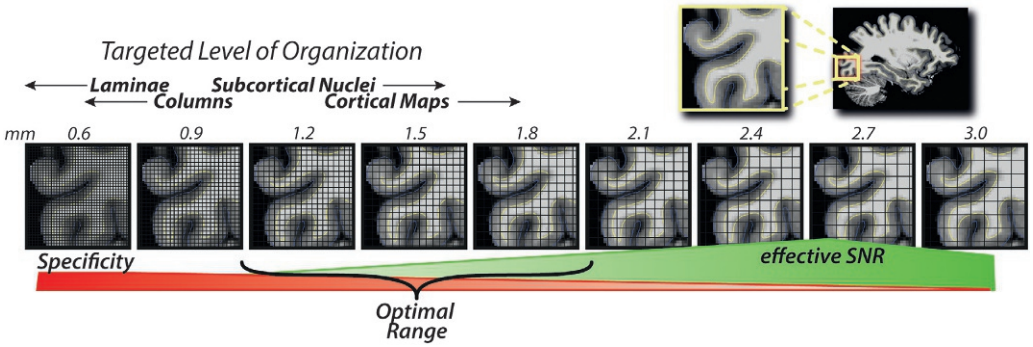

FIG. 25.1

Optimal resolution depends on the required spatial specificity and effective SNR. Pushing for higher resolution sacrifices effective SNR. We argue that for cognitive neuroscience, the optimal range for this trade-off is intermediate and advocates the use of voxel sizes that optimize sampling of BOLD responses from gray matter, i.e., gray-matter optimized fMRI. This approach capitalizes increases in both specificity and effective SNR at UHF relative to lower-field imaging. This measurement strategy has already proven highly effective in answering fundamental questions about brain organization by allowing the sampling of local neuronal population responses at UHF.

The inherent increase in fMRI signal sensitivity and specificity at UHF presents the possibility of increasing spatial resolution and moving leftward on the continuum depicted in Fig. 25.1. For typical cognitive neuroscience experiments, one should refrain from moving to submillimeter "laminar" resolution fMRI (see Box 25.2). These resolutions often yield lower effective sensitivity than traditional whole-brain 3T measurements. Instead, by moving to what we coin ***gray-matter optimized (GMO) fMRI***, intermediate voxel sizes between 1 and 2 mm isotropic, one can already benefit greatly in a variety of mutually enhancing ways. Crucially, GMO resolutions are more likely to retain a marked improvement in BOLD sensitivity relative to 3T, not only in the cerebral cortex (van der Zwaag et al., 2009), but also in the cerebellar cortex and the subcortex (Colizoli et al., 2021). As its name implies, GMO sampling is more likely to draw BOLD signals specifically from gray matter than larger, traditional voxels. This resolution reduces partial voluming effects with white matter, veins, or cerebrospinal fluid (Viessmann and Polimeni, 2021). This resolution also decreases the probability that single voxels sample from the two opposite banks of a sulcus, improving the specificity of functional localization. Moreover, the co-registration of functional images with anatomy improves, due to the increased anatomical detail at GMO resolutions. GMO fMRI decreases distortions induced by B_0 inhomogeneity, while simultaneously improving their post-hoc correction. When GMO voxels are subsequently averaged across cortical depth, this further improves the BOLD sensitivity of the resulting surface-based functional data. Last, this approach still allows whole-brain coverage, including the cerebellum, at a reasonable sample rate of at least every two seconds (0.5 Hz). This temporal resolution improves the ability to perform nuisance regression, further enhancing effective sensitivity relative to the low temporal resolutions ($<$0.5 Hz) often used in higher resolutions.

In addition to these technical reasons for GMO sampling, there is a fundamental neuroscientific reason for the focus of GMO fMRI on the organization of the brain along the cortical surface. Because

the cerebral cortex consists of intertwined hierarchies of maps on the surface of the cerebral cortex, this surface, sampled at the millimeter scale, constitutes a naturally appropriate level of detail for the study of cognitive brain function. The fact that GMO fMRI at UHF can sample the entire brain without sacrificing coverage accords well with this focus. The high-fidelity sampling of local neuronal population activations can thus be achieved while researchers need to adopt only minor changes to their traditional preprocessing and analysis approaches. We argue that for cognitive neuroscience, gray-matter optimized sampling represents a perfect combination of the desired precision and the precision that is practically attainable.

25.3 Moving toward individualized cognitive neuroscience

To highlight the promise of UHF for cognitive neuroscience experiments, we will first sketch the approach taken by the majority of current cognitive neuroimaging studies. Standard practice for functional MRI as it has evolved over the last two decades is to perform multiparticipant experiments. The typical 3T fMRI sequence scans the entire brain using about 2–4 mm isotropic voxels every 1–2 s or so (TR) for roughly 5–10 several minutes. This fMRI sequence is repeated multiple times for about an hour, in which participants perform cognitive tasks. These functional acquisitions are supplemented by a T_1-weighted anatomy at ~1-mm resolution, and possibly several types of scans intended to aid in preprocessing of the data. During preprocessing, the functional data are registered to the anatomy, often smoothed spatially, and the anatomy is coregistered to a volumetric standard-brain atlas (Collins et al., 1994). A more sophisticated way of alignment across participants is to reconstruct the cortical surfaces from the anatomy. Sampling the functional data to these surfaces honors the sheet-like anatomical structure of the cerebral cortex. The surfaces can be aligned to a surface-defined atlas. Both volumetric and surface-based atlases provide a common spatial reference frame for all participants in a given study, and also allow cross-experiment comparison of results. These results are often displayed as clusters of across-participants, mixed-effects statistical values, for example, of a GLM analysis contrast comparing experimental conditions.

There are a number of assumptions in this general approach. First, that neural tissue responds homogeneously enough throughout a brain region so that fMRI results from clusters of voxels with identical responses. That is, larger clusters or regions—and not the local neural populations sampled by single voxels—are the assumed unit of function or measurement. This assumption may misguide researchers to think in quasi-phrenological structure–function relationships with limited focus on explicit computational mechanisms: "brain region X does Y." Moreover, this assumption is known to be false for virtually all well-described brain regions, such as primary visual and motor cortices. Second, this approach assumes that the alignment of individual participants' brains into a standard geometric space based on anatomical features aligns the participants' functional organization, such that fMRI responses can be averaged in this common space. This second assumption might be sensible for brain regions with low inter-individual variability such as primary sensory and motor regions in the cerebral cortex, or subcortical regions that are precisely localizable based on anatomical details. However, inter-individual variability increases when moving from primary regions toward those regions responsible for higher-order cognitive processes, invalidating the practice of across-participant averaging. For example, one of the historically most studied nonprimary cortical areas, visual area V5 or MT, is about 1 by 2 cm in size, and its position is on average 1 cm in any direction along the cortex from an anatomical landmark based on sulcal folding patterns (Dumoulin et al., 2000). The variation in position after perfect anatomical alignment is thus as large as the area itself. Last, the likelihood of these

assumptions to be valid may be even worse if we move toward psychiatric and neurological disorders, and it is likely that the problems with these assumptions stand in the way of productive applications of fMRI in the clinical domain.

Recently, several investigators have called for the averaging of more participants in order to increase statistical power and, ultimately, replicability. However, statistical power depends not only on the number of participants but also on both the number of participants and the number of measurements (and their quality) per participant (Baker et al., 2020). The latter is often ignored but equally important. UHF fMRI increases the measurement power at the participant level, thereby shifting the balance toward within-participant experimentation. As within-participant results improve, the across-participant variance is likely not dominated by variations in function, but by limitations of volumetric and surface-based alignment. That is, individuals differ and likewise brains differ. A clear example for this is the visual system. The primary visual cortex varies in size by a factor 2–3 with relatively minor perceptual consequences.

We argue that in order to harness the power of UHF, either more sophisticated alignment methods are needed that respect the functional anatomy, or alignment is circumvented altogether. The latter can be achieved by the use of ROI-based averaging, or not averaging at all if signals are strong enough to reach statistical significance per participant. UHF provides the power to achieve statistical significance per participant, using multiple participants as replication units rather than measurement units.

An example of more sophisticated alignment is the open resource of the human connectome project (HCP) 7T fMRI dataset of 181 individual participants (Essen et al., 2013). The surface-based alignment is based upon cortical folding, cortical myelin distribution, functional resting state connectivity, and mapping data. This experiment resulted in high-quality maps of visual space in early visual cortex, visual thalamus and superior colliculus (Benson et al., 2018), and tonotopic maps in early auditory cortex (Hedger and Knapen, 2021), but has also lead to discoveries of maps of visual space outside the traditional visual cortex: in the hippocampus (Knapen, 2021; Silson et al., 2021), default mode network (Szinte and Knapen, 2020), and cerebellum (van Es et al., 2019) (see Fig. 25.2, cf. (Groen et al., 2021)). At brain locations that are less consistent across individuals, such as is the case in higher-level visual regions in occipital, parietal, and frontal cortex, this across-participant averaging is problematic. Specifically, for maps of visual space, it is likely to lead to (a) an under-estimation of the strength of visually tuned responses because we will average out relevant signals instead of noise and (b) an unpredictable effects on the precise tuning that is found, making these results hard to interpret. We note that this is not a problem specific to visual processing. Rather, it is a specific instance of the above-mentioned problem that alignment across individuals based on anatomical landmarks does not guarantee alignment of functional organization. In regions with appreciable across-individual variability (the better part of the cerebral cortex), we are therefore forced to go to the level of the single individual.

UHF fMRI compels us to confront the above-mentioned assumptions and allows us to challenge them. Its increased sensitivity and specificity allow UHF fMRI to fulfill its promise as a tool for the measurement of local neural population activity, and as a tool for a cognitive neuroscience that rightfully values the uniqueness of individuals' brain structure and function, thereby encouraging researchers to focus on individual participants and local neural computations.

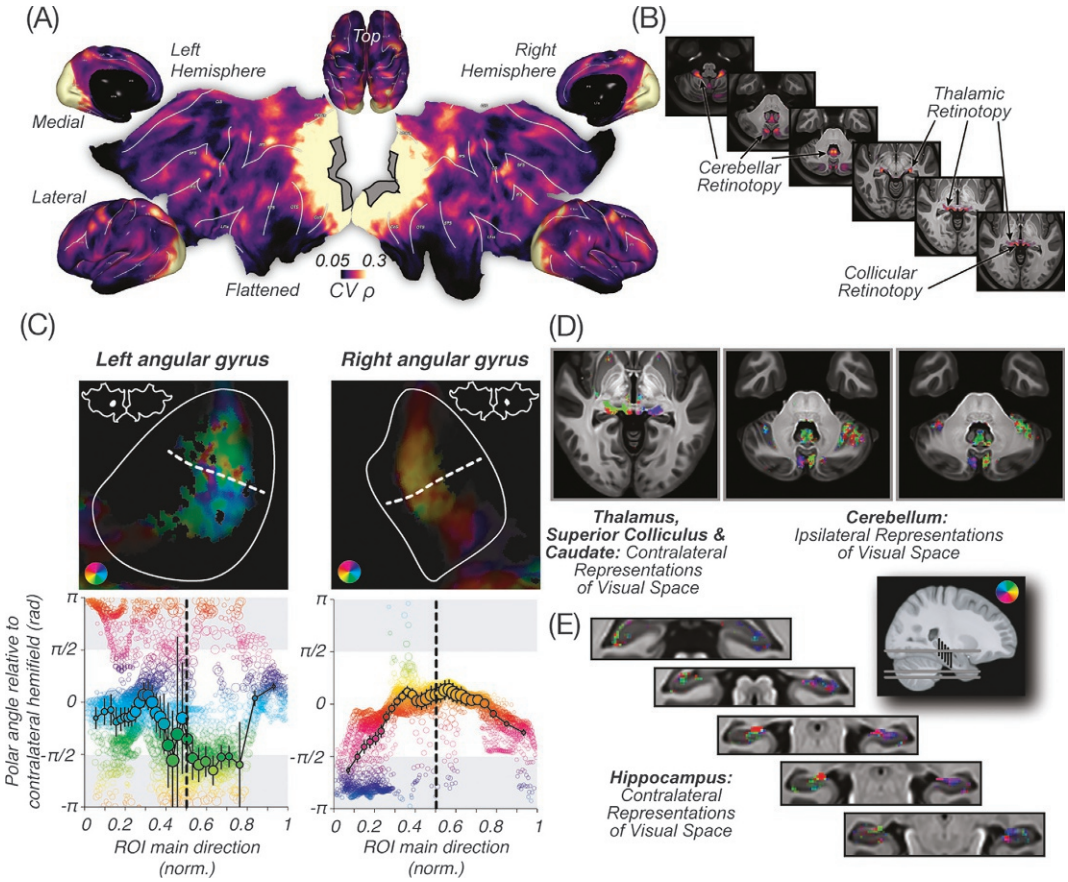

FIG. 25.2

GMO fMRI has revealed tuning for visual location for beyond the occipital lobe, i.e., visual population receptive fields and connective fields. (A) Distribution of cross-validated variance explained by connective fields on the flattened cerebral cortex. (B) Distribution of variance explained in the subcortex, same quantification as in (A). (C) Map-like structure of population receptive fields in the default mode network. Color denotes preferred polar angle: the direction in the visual field independent of visual eccentricity. These regions represent contralateral visual space. (D) Population receptive field polar angle position throughout the subcortex, in thalamus, superior colliculus, caudate nucleus, and cerebellum. As in the traditional visual system and default mode network, subcortical visual responses in these regions reflect contralateral visual space except cerebellum. Cerebellum features ipsilateral visual field representations, in line with its ipsilateral somatotopic maps. (E) Polar angle distribution in hippocampus, showing a detailed pattern of contralateral visual field preference. *Based on Groen et al. (2021).*

25.4 Respecting local neural populations: Human systems neuroscience at UHF

One of the previously considered assumptions is that neural tissue responds homogeneously enough throughout a brain region, so that fMRI results from clusters of voxels with identical responses. However, none of the most well-described cortical regions have homogeneous responses throughout what is considered a homogeneous area. For example, within the primary visual cortex (V1), different parts respond to different locations in the visual field, and V1 function differs drastically between central and peripheral visions. Despite these differences, V1 is indeed homogenous in its implementation of fixed computational principles. The same holds for early visual cortex in general, and other sensory and motor cortices: Although exact tuning varies drastically within regions, computational principles do not. We contend that this is likely the case for the brain in general; therefore, we suggest that the underlying assumption should not be that an area responds homogeneously, but that responses in an area reflect coherent computational principles.

There are several types of analysis that respect local neural populations as reflected in single time courses of individual voxels, for example, multivoxel pattern analysis and single-time-course modeling. For example, single-time-course modeling has been used to great effect even at 3T, with encoding-model analysis capturing receptive field properties of the sampled neuronal population (Dumoulin and Wandell, 2008; Kay et al., 2008) and, for example, revealing the brain's semantic organization (Huth et al., 2016). These types of experiments can readily benefit from UHF as they already focus on high SNR measurements on individual participants (Gratton

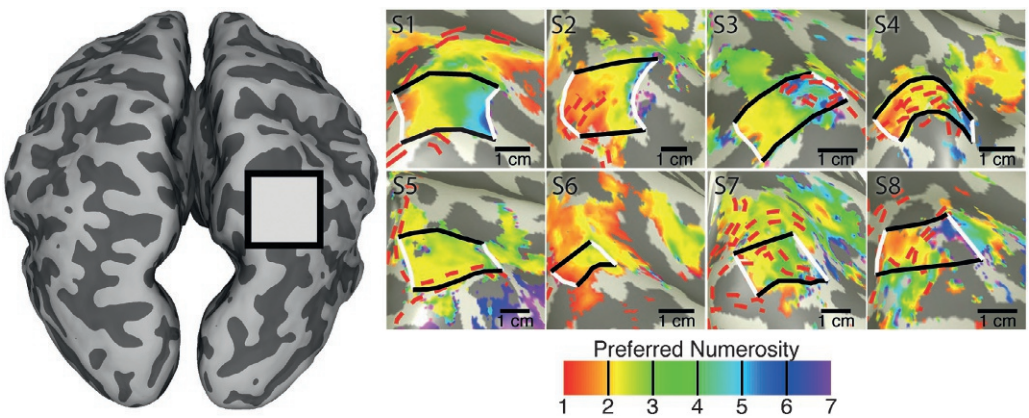

FIG. 25.3

Example of across-participant variability of cortical organization in the cerebral cortex. Topographic maps of numerosity preference are shown for eight participants, zoomed into the portion of the brain highlighted on the left. There is a topographic map in each of the participants at the same approximate location and approximate orientation, but the exact tuning at each location varies widely. Averaging this tuning across participants in a common anatomical space would drastically dilute this information tuning. *Based on Harvey et al. (2013).*

et al., 2022). A recent initiative, the natural scenes dataset (Allen et al., 2021), provides a beautiful example of how GMO UHF fMRI can be leveraged at the unique individual level. In this project, 8 participants were scanned for 30–40 sessions each while viewing up to 10,000 natural images on which they performed an image-recognition task. With GMO single-voxel responses to this amount of stimuli, this is an invaluable resource with a unique focus on high-SNR measurements in individual participants.

One of the earliest discoveries using UHF in the field of cognitive neuroscience was the topographic maps that represent dimensions of numerical cognition. First, the discovery of maps that systematically represents numerosity akin to a mental number line (Harvey et al., 2013), followed by cognitive topographic maps that represent object size (Harvey et al., 2015), time duration (Protopapa et al., 2018), and haptic numerosity (Hofstetter et al., 2021). These discoveries suggest that topographic principles common in primary sensory and motor cortices may also be an organizing principle of cognitive functions in association cortex. Fig. 25.3 demonstrates that these human numerosity maps vary strongly between individuals in terms of their precise location and orientation—again highlighting the necessity of performing these analyses at the single-participant level.

These numerosity maps have been used to showcase the strength of UHF relative to standard field strength acquisitions. We compared the relative efficacy of 3T and 7T acquisitions in charting these numerosity maps in single individuals (Cai et al., 2021), and showed that for every run acquired at 7T, one would need to acquire approximately four runs at 3T to attain the same variance explained or effective SNR (see Fig. 25.4).

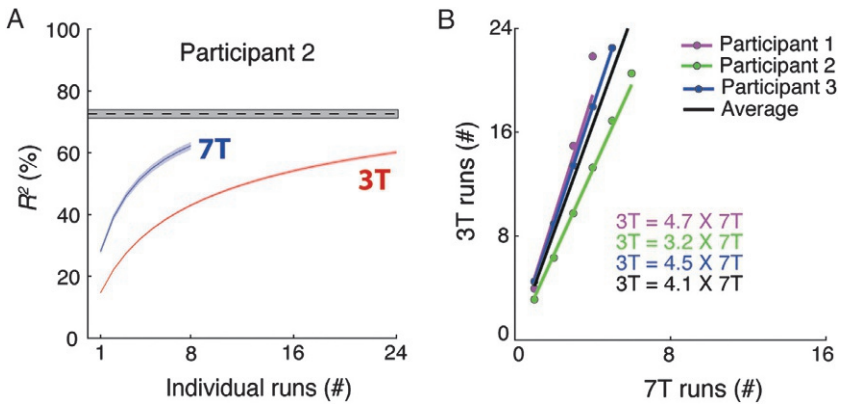

FIG. 25.4

The amount of data needed for a given variance explained (R2) at 3T is roughly four times the amount of data needed at 7T. (A). Test–retest reliability as a function of number of runs averaged, expressed as cross-validated R2. These data were acquired in a numerosity-mapping experiment (Fig. 25.3). Curves show the amount of runs needed to approach the noise ceiling for a single participant. 8 runs of 7T data have higher cross-validated R2 than 24 runs of 3T data. (B). The amount of 3T runs that equal the amount of 7T runs for 3 participants: Only about a quarter of the data is needed at 7T to reach the same variance explained as at 3T. *Based on Cai et al. (2021).*

25.5 Outlook

UHF fMRI optimized to sample gray-matter responses can be performed with whole-brain coverage, and analyzed using well-established analytical tools. This high degree of accessibility combined with the very high level of attainable data quality makes GMO fMRI a very compelling strategy for cognitive neuroscience. GMO fMRI's specific sampling of local neuronal population activations allows it to probe computational principles at work in the living human brain. This allows UHF fMRI to bridge cognitive neuroscience, neurophysiology in animal models, and computational neuroscience, with a unique focus on high-SNR measurements in individual participants. Since specific deficits in computational processes characterize many psychiatric disorders, GMO fMRI also holds promise for the eventual use of fMRI for clinical purposes.

References

Allen, E.J., St-Yves, G., Wu, Y., et al., 2021. A massive 7T fMRI dataset to bridge cognitive neuroscience and artificial intelligence. Nat. Neurosci. 1–11. https://doi.org/10.1038/s41593-021-00962-x.

Baker, D.H., Vilidaite, G., Lygo, F.A., et al., 2020. Power contours: optimising sample size and precision in experimental psychology and human neuroscience. Psychol. Methods 26, 295–314. https://doi.org/10.1037/met0000337.

Benson, N.C., Jamison, K.W., Arcaro, M.J., et al., 2018. The Human Connectome Project 7 Tesla retinotopy dataset: description and population receptive field analysis. J. Vis. 18, 23. https://doi.org/10.1167/18.13.23.

Brodmann, K., 1909. In: Brodmann, K. (Ed.), Vergleichende Lokalisationslehre der Grosshirnrinde in ihren Prinzipien dargestellt auf Grund des Zellenbaues von Dr. J.A. Barth.

Caan, M.W.A., Bazin, P., Marques, J.P., Hollander, G., Dumoulin, S.O., Zwaag, W., 2018. MP2RAGEME: T1, T2*, and QSM mapping in one sequence at 7 tesla. Hum. Brain Mapp. https://doi.org/10.1002/hbm.24490.

Cai, Y., Hofstetter, S., van der Zwaag, W., Zuiderbaan, W., Dumoulin, S.O., 2021. Individualized cognitive neuroscience needs 7T: Comparing numerosity maps at 3T and 7T MRI. Neuroimage 237, 118184. https://doi.org/10.1016/j.neuroimage.2021.118184.

Colizoli, O., de Gee, J.W., van der Zwaag, W., Donner, T.H., 2021. Functional magnetic resonance imaging responses during perceptual decision-making at 3 and 7 T in human cortex, striatum, and brainstem. Hum. Brain Mapp. 43, 1265–1279. https://doi.org/10.1002/hbm.25719.

Collins, D.L., Neelin, P., Peters, T.M., Evans, A.C., 1994. Automatic 3D intersubject registration of MR volumetric data in standardized talairach space. J. Comput. Assist. Tomogr. 18, 192–205. https://doi.org/10.1097/00004728-199403000-00005.

Dumoulin, S.O., Wandell, B.A., 2008. Population receptive field estimates in human visual cortex. Neuroimage 39, 647–660.

Dumoulin, S.O., Bittar, R.G., Kabani, N.J., et al., 2000. A new anatomical landmark for reliable identification of human area V5/MT: a quantitative analysis of sulcal patterning. Cereb. Cortex 10, 454–463. https://doi.org/10.1093/cercor/10.5.454.

Essen, D.C.V., Smith, S.M., Barch, D.M., Behrens, T.E.J., Yacoub, E., Ugurbil, K., 2013. The WU-Minn human connectome project: an overview. Neuroimage 80 (62), 79. https://doi.org/10.1016/j.neuroimage.2013.05.041.

Felleman, D.J., Essen, D.C.V., 1991. Distributed hierarchical processing in the primate cerebral cortex. Cereb. Cortex 1 (1), 47. https://doi.org/10.1093/cercor/1.1.1.

Fracasso, A., van Veluw, S.J., Visser, F., et al., 2016. Lines of Baillarger in vivo and ex vivo: Myelin contrast across lamina at 7T MRI and histology. Neuroimage 133, 163–175. https://doi.org/10.1016/j.neuroimage.2016.02.072.

Gratton, C., Nelson, S.M., Gordon, E.M., 2022. Brain-behavior correlations: two paths toward reliability. Neuron 110, 1446–1449. https://doi.org/10.1016/j.neuron.2022.04.018.

Groen, I.I.A., Dekker, T.M., Knapen, T., Silson, E.H., 2021. Visuospatial coding as ubiquitous scaffolding for human cognition. Trends Cogn. Sci. https://doi.org/10.1016/j.tics.2021.10.011.

Harvey, B.M., Klein, B.P., Petridou, N., Dumoulin, S.O., 2013. Topographic representation of numerosity in the human parietal cortex. Science (New York, NY) 341, 1123–1126. https://doi.org/10.1126/science.1239052.

Harvey, B.M., Fracasso, A., Petridou, N., Dumoulin, S.O., 2015. Topographic representations of object size and relationships with numerosity reveal generalized quantity processing in human parietal cortex. Proc. Nat. Acad. Sci. 112, 13530. https://doi.org/10.1073/pnas.1515414112.

Hedger, N., Knapen, T., 2021. Naturalistic audiovisual stimulation reveals the topographic organization of human auditory cortex. Biorxiv. https://doi.org/10.1101/2021.07.05.447566.

Hofstetter, S., Cai, Y., Harvey, B.M., Dumoulin, S.O., 2021. Topographic maps representing haptic numerosity reveals distinct sensory representations in supramodal networks. Nat. Commun. 12, 221. https://doi.org/10.1038/s41467-020-20567-5.

Horton, J.C., Adams, D.L., 2005. The cortical column: a structure without a function. Philos. Trans. Roy. Soc. B Biol. Sci. 360, 837–862. https://doi.org/10.1098/rstb.2005.1623.

Hubel, D.H., Wiesel, T.N., 1977. Ferrier lecture—functional architecture of macaque monkey visual cortex. Proc. R. Soc. Lond. B Biol. Sci. 198, 1–59. https://doi.org/10.1098/rspb.1977.0085.

Huth, A.G., de Heer, W.A., Griffiths, T.L., Theunissen, F.E., Gallant, J.L., 2016. Natural speech reveals the semantic maps that tile human cerebral cortex. Nature 532 (453), 458. https://doi.org/10.1038/nature17637.

Jones, E.G., Burton, H., Porter, R., 1975. Commissural and cortico-cortical "Columns" in the somatic sensory cortex of primates. Science 190, 572–574. https://doi.org/10.1126/science.810887.

Kay, K.N., Naselaris, T., Prenger, R.J., Gallant, J.L., 2008. Identifying natural images from human brain activity. Nature 452, 352–355.

Knapen, T., 2021. Topographic connectivity reveals task-dependent retinotopic processing throughout the human brain. Proc. Nat. Acad. Sci. 118, e2017032118. https://doi.org/10.1073/pnas.2017032118.

Mountcastle, V.B., Davies, P.W., Berman, A.L., 1957. Response properties of neurons of cat's somatic sensory cortex to peripheral stimuli. J. Neurophysiol. 20, 374–407. https://doi.org/10.1152/jn.1957.20.4.374.

Protopapa, F., Hayashi, M., Kulashekhar, S., et al., 2018. Chronotopic maps in human medial premotor cortex. Biorxiv. https://doi.org/10.1101/399857.

Silson, E.H., Zeidman, P., Knapen, T., Baker, C.I., 2021. Representation of contralateral visual space in the human hippocampus. J. Neurosci. 41, 2382–2392. https://doi.org/10.1523/jneurosci.1990-20.2020.

Stanley, J.A., Raz, N., 2018. Functional magnetic resonance spectroscopy: the "New" MRS for cognitive neuroscience and psychiatry research. Front. Psych. 9, 76. https://doi.org/10.3389/fpsyt.2018.00076.

Szinte, M., Knapen, T., 2020. Visual organization of the default network. Cereb Cortex New York N Y 1991 (30), 3518–3527. https://doi.org/10.1093/cercor/bhz323.

Trampel, R., Ott, D.V.M., Turner, R., 2011. Do the congenitally blind have a stria of Gennari? First intracortical insights in vivo. Cereb. Cortex 21, 2075–2081. https://doi.org/10.1093/cercor/bhq282.

Uludağ, K., Müller-Bierl, B., Uğurbil, K., 2009. An integrative model for neuronal activity-induced signal changes for gradient and spin echo functional imaging. Neuroimage 48, 150–165.

van der Zwaag, W., Francis, S., Head, K., et al., 2009. fMRI at 1.5, 3 and 7 T: characterising BOLD signal changes. Neuroimage 47, 1425–1434. https://doi.org/10.1016/j.neuroimage.2009.05.015.

van Es, D.M., van der Zwaag, W., Knapen, T., 2019. Topographic maps of visual space in the human cerebellum. Curr. Biol. 29, 1689–1694.e3. https://doi.org/10.1016/j.cub.2019.04.012.

Viessmann, O., Polimeni, J.R., 2021. High-resolution fMRI at 7Tesla: challenges, promises and recent developments for individual-focused fMRI studies. Curr. Opin. Behav. Sci. 40, 96–104. https://doi.org/10.1016/j.cobeha.2021.01.011.

Vogt, C., Vogt, O., 1919. Allgemeine Ergebnisse unserer Hirnforschung. J. Psych. Neurol. 25 (J.A. Barth).

Weiskopf, N., Suckling, J., Williams, G., et al., 2013. Quantitative multi-parameter mapping of R1, PD*, MT, and R2* at 3T: a multi-center validation. Front. Neurosci. 7, 95. https://doi.org/10.3389/fnins.2013.00095.

Yacoub, E., Shmuel, A., Pfeuffer, J., et al., 2001. Imaging brain function in humans at 7 Tesla. Magn. Reson. Med. 45, 588–594. https://doi.org/10.1002/mrm.1080.